Transient currents in a molecular photo-diode

E.G. Petrov [a,*], V.O. Leonov [a], V. May [b], P. Hänggi [c]

[a] Bogolyubov Institute for Theoretical Physics, National Academy of Sciences of Ukraine, Metrologichna Street 14-b, UA-03680 Kiev, Ukraine
[b] Institut für Physik, Humboldt Universität zu Berlin, Newtonstrasse 15, D-12489 Berlin, Germany
[c] Institut für Physik, Universität Augsburg, Universitätstrasse 1, D-86135 Augsburg, Germany

1. Introduction

The use of molecular nanostructures as diodes, transistors, switches, etc. is considered as one possible way towards a further miniaturization of integrated circuits. Although pioneering ideas in this direction have been formulated more than 30 years ago [1,2] the detection of current–voltage characteristics of a single molecule became only possible within the last 15 years (for an overview see [3–10]). Up to date research still mainly focuses on an understanding of charge transmission in the junction "electrode1–molecule–electrode2" (**1**-M-**2** system) where a single molecule exhibits itself as an electron/hole transmitter. It has been shown that at definite conditions the molecule is able to operate as a molecular diode. For instance, during a coherent (elastic) electron tunneling in the biased **1**-M-**2** system, diode properties of the molecule appear only in the presence of a voltage drop across the molecule. This conclusion is valid even at different contacts of the molecule with the electrodes [11]. But, if an electron transmission is associated with incoherent electron transfer processes (inelastic tunneling or/and hopping), the molecular diode can originate from an unequal coupling of the molecule to the electrodes. Just such a situation is considered in the present paper. We show that a rectification effect can be observed even in the unbiased **1**-M-**2** system where the driving force of the electron transfer process is caused by a photo excitation of the molecule.

Recent research addressed the use of organic molecules in molecular photo devices like photo-diodes, photo-resistors, optical switches, and photo-amplifiers [12,13]. For example, a light-controlled conductance switch based on a photochromic molecule has been demonstrated [14]. Moreover, single molecule luminescence caused by the current through a molecular junction could be detected [15–18].

Theoretical estimates on the light-induced current and current-induced light emission one can find in [19–25]. It has been shown that a *dc*-current can be induced by an external *ac*-field either due to a considerable difference between the electronic charge distributions within the molecular orbitals (MOs), or if the amplitude of the electric field along one direction is larger than in the opposite direction. The latter effect can be originated by a mixing of two laser pulses with frequencies ω and 2ω [21,26–29]. The generation of a *dc*-current can be also achieved by an asymmetric distribution of molecular energy levels caused by environmental fluctuations (such an asymmetry may induce a ratchet current [30]). Besides the formation of a steady-state current due to an optical excitation of the junction in the absence of an applied voltage, a light-induced suppression of a current in the presence of an applied voltage has been suggested as well [31,32]. Note also the work on a light-induced removal of the Franck–Condon blockade in a single-electron inelastic charge transmission [33].

While the examples mentioned above focus on steady-state properties of the junction, also the formation of transient currents generated just after an alteration of the applied voltage or by changing optical excitation attracted recent interest. The computations demonstrated that the transient current in a molecular diode appearing just after a sudden voltage switch-on or switch-off can significantly exceed the steady-state value [34,38]. Such a behavior is caused by electron transfer processes which are responsible for charging or discharge of the molecule and which are fast compared to the processes that establish the steady state current.

* Corresponding author.
E-mail address: epetrov@bitp.kiev.ua (E.G. Petrov).

It is the objective of the present work to study the time-dependent behavior of the transient current across a molecular junction in the absence of an applied voltage. In doing so we focus on the transient current formed just after a fast switch-on of a *cw*-optical excitation. Our analysis allows to clarify the physical mechanisms which are responsible for the fast and the slow kinetic phases of charge transmission through the molecular junctions.

The paper is organized as follows. General expressions for the sequential (hopping) and direct (tunnel) current components in a molecular junction are given in Section 2 along with the kinetic equations for the molecular state populations and respective transfer rates. In Section 3, a HOMO–LUMO description of the molecule is introduced to derive concrete expressions for contact as well as inelastic tunnel rates. Expressions for the transient photocurrent are presented in Section 4. In Section 5, the results related to the off-resonant and the resonant regime of current formation are discussed in details. Some concluding remarks are presented in Section 6.

2. Basic equations

2.1. Hamiltonian

We introduce a model of the **1**-M-**2** molecular junction formed by two nonmagnetic electrodes which are weakly coupled to the (nonmagnetic) molecule. The related Hamiltonian of the system can be written as

$$H = H_e + H_m + H' + H_f(t). \tag{1}$$

The first term describes the Hamiltonian of the ideal electrodes,

$$H_e = \sum_{r\mathbf{k}\sigma} E_{r\mathbf{k}} a^+_{r\mathbf{k}\sigma} a_{r\mathbf{k}\sigma}, \tag{2}$$

where $E_{r\mathbf{k}}$ denotes the energy of a conduction band electron (with wave vector $\mathbf{k}$) of the $r(=1,2)$th electrode. For nonmagnetic electrodes and in the absence of a magnetic field this energy does not depend on the electron spin σ. Electron creation and annihilation operators are denoted by $a^+_{r\mathbf{k}\sigma}$ and $a_{r\mathbf{k}\sigma}$, respectively. The expression

$$H_m = \sum_{M(N)} E_{M(N)} |M(N)\rangle\langle M(N)| \tag{3}$$

defines the Hamiltonian of the molecule, where $E_{M(N)}$ denotes the energy of the molecule in state $|M(N)\rangle$. The quantum number M labels the actual electronic, vibrational, and spin state of the molecule; N denotes the number of electrons in the molecule. The third term in Eq. (1) reads

$$H' = \sum_{r\mathbf{k}\sigma} \sum_{N,MM'} \left[V_{M'(N+1);r\mathbf{k}\sigma M(N)} \times |M'(N+1)\rangle\langle M(N)| a_{r\mathbf{k}\sigma} + h.c. \right]. \tag{4}$$

It describes the molecule–electrode interaction with the matrix element $V_{M'(N+1);r\mathbf{k}\sigma M(N)} = \langle M'(N+1)|V_{tr}|r\mathbf{k}\sigma M(N)\rangle$ characterizing the electron exchange (V_{tr} is the electron transfer operator). The interaction of the molecule with an external *cw*-field is written in the standard form

$$H_f(t) = -\mathbf{E}(t) \sum_{MM'N} \mathbf{d}_{M'M} |M'(N)\rangle\langle M(N)|, \tag{5}$$

where $\mathbf{E}(t)$ is the electric component of the periodic field and $\mathbf{d}_{M'M}$ is the transition dipole matrix element between different states of the molecule.

2.2. Sequential and direct components of an electron current

The current across the electrode r is given by

$$I_r(t) = e(\delta_{r,1} - \delta_{r,2})\dot{N}_r(t), \tag{6}$$

where $e = -|e|$ is the electron charge, $\dot{N}_r(t) = \sum_{\mathbf{k}\sigma} \dot{P}(r\mathbf{k}\sigma; t)$ denotes the electron flow from the rth electrode, and $P(r\mathbf{k}\sigma; t)$ is the population of the single-electron band state. For stationary charge transmission the number of electrons leaving one of the electrodes is identical with the number of electrons arriving at the other electrode, i.e. $\dot{N}_1(t) = -\dot{N}_2(t) = const$. In the nonstationary regime, however, $\dot{N}_1(t)$ and $\dot{N}_2(t)$ may be quite different from each other so that $I_1(t) \neq I_2(t)$ (cf. Refs. [34,38]).

Nonequilibrium density matrix (NDM) theory [35–37] is quite suitable to achieve a unified description of elastic (coherent) as well as inelastic (hopping and incoherent) charge transmission in the molecular junctions. Such description allows one to express the transfer rates characterizing the noted transmission via the set of molecule–electrode couplings and transmission gaps. In Refs. [38–42], the NDM theory has been used to derive kinetic equations for the single electron populations $P(r\mathbf{k}\sigma; t)$ and the molecular populations $P(M(N); t)$. Just these equations determine the evolution of the current components in the molecular junctions.

In the presence of an external *cw*-field, the derivation procedure becomes more complicated. If, however, the interaction, Eq. (5), acts as a perturbation only, the calculation of electron transfer rates associated with the interaction, Eq. (4), can be carried out by ignoring the molecule–field interaction. The condition that permits one to consider the interaction (5) as a perturbation, reduces to the inequality

$$\omega^2 \gg |\mathbf{E}\mathbf{d}_{M'M}|^2/\hbar^2 \tag{7}$$

where $|\mathbf{E}|$ is the amplitude of the *cw*-field. Owing to the condition (7), only single photon transitions with frequency $\omega = (1/\hbar)|E_{M(N)} - E_{M'(N)}|$ will support charge transfer processes in the **1**-M-**2** device. The derivation of kinetic equations for the populations $P(r\mathbf{k}\sigma; t)$ and $P(M(N); t)$ remains identical with that already presented in [38–42]. Therefore, we do not repeat the derivation here. We only mention that for the considered weak molecule–electrode coupling a unified description of charge transmission is achieved by using the transition operator $\widehat{T} = H' + H'\widehat{G}(E)H'$ (note that the electrodes stay in equilibrium). The matrix elements $\langle a|\widehat{T}|b\rangle$ determine the transitions between the states b and a on the energy shell $E = E_a = E_b$ [43], where the E_a and E_b are energies referring to the Hamiltonian $H_0 = H_e + H_m$. The Green's operator $\widehat{G}(E) = (H_0 + H' + i0^+)^{-1}$ is defined by the Hamiltonian of the whole **1**-M-**2** system in the absence of molecule–field interaction. The first term of $\widehat{T}$ is responsible for a single electron hopping between the molecule and the attached electrodes while the second term results in a direct one-step electron transition between the electrodes. Besides, the operator $H'\widehat{G}(E)H'$ is responsible for a specific electron–pair transition between the molecule and the electrodes. Respective transfer rates are presented in Refs. [38,42]. The mechanism of electron-pair transitions has been applied earlier to explain the nonlinear electron transport through a single-level quantum dot [44]. For such a transport the repulsion between the transferred electrons in the dot is compensated by the voltage bias. In the present paper, a light-induced charge transmission is considered in an unbiased molecular junction. Therefore, the energies of twofold charged molecular states are arranged high enough to only give a negligible contribution to the current. It means that the pair-electron transfer processes become unimportant and, thus, our study is limited to single electron transmission processes. As a result, the current through the rth electrode has two components

$$I_r(t) = I^{(r)}_{seq}(t) + I_{dir}(t). \tag{8}$$

The sequential component,

$$I^{(r)}_{seq}(t) = |e|(-1)^{r+1}\sum_{N,MM'}\left(\chi^{(r)}_{M(N)\to M'(N+1)} - \chi^{(r)}_{M(N)\to M'(N-1)}\right)P(M(N);t) \tag{9}$$

is defined by single electron jumps through the contact region between the electrode surface and the molecule. Respective hopping transfer rates can be referred to the contact forward (electrode–molecule) and contact backward (molecule–electrode) rates which read

$$\chi^{(r)}_{M(N)\to M'(N+1)} = \frac{2\pi}{\hbar}\sum_{\mathbf{k}\sigma}|V_{M'(N+1);r\mathbf{k}\sigma M(N)}|^2 \times f_r(E_{r\mathbf{k}})\delta\left[E_{r\mathbf{k}} + E_{M(N)} - E_{M'(N+1)}\right] \tag{10}$$

and

$$\chi^{(r)}_{M(N)\to M'(N-1)} = \frac{2\pi}{\hbar}\sum_{\mathbf{k}\sigma}|V_{M'(N-1)r\mathbf{k}\sigma;M(N)}|^2 \times [1 - f_r(E_{r\mathbf{k}})]\delta[E_{r\mathbf{k}} + E_{M'(N-1)} - E_{M(N)}]. \tag{11}$$

[In Eqs. (10) and (11), $f_r(E_{r\mathbf{k}}) = \{\exp[(E_{r\mathbf{k}} - \mu_r)/k_BT] + 1\}^{-1}$ is the Fermi distribution function with μ_r being the chemical potential for the rth electrode.] Contact forward and backward rates are responsible, respectively, for reduction and oxidation of the molecule by the rth electrode. In mesoscopic physics, a similar type of hopping processes is classified as an electron tunneling between the lead and the dot [45].

The current component

$$I_{dir}(t) = |e|\sum_{N,MM'} S^{(dir)}_{MM'}(N)P(M(N);t) \tag{12}$$

is formed by an interelectrode electron transfer at which the molecule mediates a charge transmission without alteration of its charge. Such process is defined by the electron flows

$$S^{(dir)}_{MM'}(N) = Q_{1M(N)\to 2M'(N)} - Q_{2M(N)\to 1M'(N)} \tag{13}$$

where the transfer rates

$$Q_{rM(N)\to r'M'(N)} = \frac{2\pi}{\hbar}\sum_{\mathbf{k}\sigma,\ \mathbf{k}'\sigma'}\sum f_r(E_{r\mathbf{k}})[1 - f_{r'}(E_{r'\mathbf{k}'})] \times |\langle M'(N)r'\mathbf{k}'\sigma'|H'\widehat{G}(E)H'|r\mathbf{k}\sigma M(N)\rangle|^2 \times \delta[E_{r\mathbf{k}} + E_{M(N)} - E_{r'\mathbf{k}'} - E_{M'(N)}], \tag{14}$$

characterize a distant electron transmission from the $\mathbf{k}\sigma$ band states of the rth electrode to the $\mathbf{k}'\sigma'$ band states of the r'th electrode. Such transmission appears as a direct single-step elastic (at $M'(N) = M(N)$) or inelastic (at $M'(N) \neq M(N)$) interelectrode electron tunneling. Since the operator H' is responsible for transitions accompanied by an alteration of molecular charge, the mediation of the tunneling transmission occurs via the formation of intermediate molecular states $\widetilde{M}(N+1)$ and $\widetilde{M}(N-1)$ which differ from the initial, $M(N)$ and final, $M'(N)$ charge states. In the contrast to the sequential (hopping) transmission where similar states are really populated, the noted intermediate states are not populated and only acts as virtual states. In mesoscopic physics, such type of transmission refers to co-tunneling [45]. In the respective terminology the direct current component, Eq. (13), results as a contribution of partial currents associated with different co-tunneling channels. The realization of a particular channel is controlled by the probability $P(M(N);t)$ to find a molecule in the $M(N)$th stay. [Examples of electron transmission along the channel pathways that include the empty and occupied MOs can be found in [46,47].] Thus, the direct tunneling can be referred to as co-tunneling which is controlled by kinetic charging and recharge of the molecule (via electron jumps through the contact region). This circumstance has been already noted in [48]. In the presence of the *cw*-field, an additional control occurs through the population of the excited molecular state.

2.3. Kinetic equations for the molecular populations

It follows from Eqs. (9) and (12) that each charge transmission route (sequential or direct) includes electron transfer channels related to the molecular states $M(N)$. The contribution of the $M(N)$th channel to the route is weighted by the molecular population $P(M(N);t)$, which satisfies the normalization condition

$$\sum_{NM} P(M(N);t) = 1. \tag{15}$$

Following the derivation procedure presented in Refs. [38,42,49] and bearing in mind the fact that the interactions (4) and (5) are considered as perturbations, we can see that evolution of the $P(M(N);t)$ is determined by the balance like kinetic equation

$$\dot{P}(M(N);t) = -\sum_{M'N'}\left[\mathcal{K}_{M(N)\to M'(N')}P(M(N);t) - \mathcal{K}_{M'(N')\to M(N)}P(M'(N');t)\right]. \tag{16}$$

The transfer rate

$$\mathcal{K}_{M(N)\to M'(N')} = \sum_r(\delta_{N',N+1} + \delta_{N',N-1}) \times \chi^{(r)}_{M(N)\to M'(N')} + \delta_{N,N'}\left[K^{(f)}_{M(N)\to M'(N)} + \sum_r(1 - \delta_{r,r'})Q_{rM(N)\to r'M'(N')}\right] \tag{17}$$

specifies the transition from the state $M(N)$ to the state $M'(N')$ in the molecule. Such transition is caused by the molecule–electrode interaction (4) through the contact and distant transfer rates (Eqs. (10), (11), (14)) as well as by the molecule–field interaction (5). Respective rates of optical excitation and de-excitation are

$$K^{(f)}_{M(N)M'(N)} = \frac{2\pi}{\hbar}|\mathbf{Ed}_{M'(N)M(N)}|^2 \times [L_{M'(N)M(N)}(\omega) + L_{M'(N)M(N)}(-\omega)]. \tag{18}$$

We introduced $L_{M'(N)M(N)}(\omega) = (1/2\pi)(\kappa_{M(N)} + \kappa_{M'(N)})\{[\hbar\omega - (E_{M'(N)} - E_{M(N)})]^2 + (\kappa_{M(N)} + \kappa_{M'(N)})^2/4\}^{-1}$, where $\kappa_{M(N)}/2$ denotes the molecular level broadening caused by electron–phonon interaction as well as interaction of the molecule with the electrodes (for more details see [49]).

3. Charge transfer processes in the HOMO–LUMO model

Next, the hopping rates, Eqs. (10) and (11) as well as the distant transfer rate, Eq. (14), all determining the net electron flow through the junction, are further specified along the rate, Eq. (18) characterizing the efficiency of excitation and de-excitation of the molecule. We use a model of the **1**-M-**2** system where only the highest occupied and the lowest unoccupied molecular orbitals (HOMO (H) and LUMO (L), respectively) are considered. The HOMO–LUMO model is suitable to study charge transmission in the molecular junctions. As an example, note the pioneer work of Aviram and Ratner [50] where the mechanism of current formation includes a participation of HOMO and LUMO levels belonging to the donor and acceptor sites of the molecule. Recently, a similar model (with chromophoric donor and acceptor sites) has been used for the description of transient dynamics in molecular junctions [51]. In this model, a transient electronic current is formed due to an optical excitation associated with the HOMO–LUMO transition in the donor site.

In the present paper, we use a model where extended HOMOs (LUMOs) are formed from HOMOs (LUMOs) belonging to the

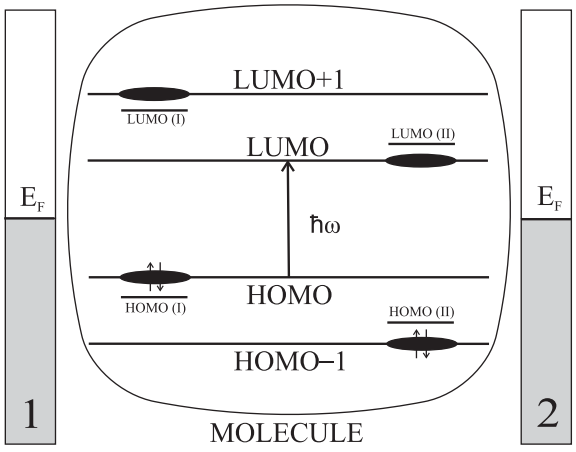

Fig. 1. Possible position of the frontier MOs in the molecule with two terminal sites I and II. Intersite coupling transforms the site MOs into extended HOMO, HOMO −1 and LUMO, LUMO +1. Spots indicate the main location of electron density within the extended MOs.

terminal molecular sites I and II coupled to one another by interior bridging groups. Let the HOMO (n) and the LUMO (n) refer to the terminal site n(=I,II). Following from the coupling between the sites, the extended HOMO and HOMO − 1 (LUMO and LUMO + 1) represent a mixture of the HOMO (I) and HOMO (II) (LUMO (I) and LUMO (II)). If the intersite coupling does not strongly modify the electron distribution across the molecule, the maxima of electron density in the HOMO, HOMO − 1, LUMO, and LUMO + 1 correspond to electron densities located in the vicinity of the respective sites, cf. Fig. 1. Therefore, the coupling of the HOMO to electrode 1 is assumed to be much stronger than the similar coupling to electrode 2. The opposite case is valid for the coupling of the LUMO to the same electrodes. This configuration as represented in Fig. 1 can be realized if, for instance, the HOMO (I)/LUMO (I) and HOMO (II)/LUMO (II) refer to the π-electrons of aromatic groups coupled to each other by the bridging σ-bonds (to avoid a noticeable mixture between the π-electrons belonging the sites I and II). If the energy $\hbar\omega$ of the external cw-field coincides with the energy of the optical HOMO–LUMO transition, then the formation of the photocurrent can be mainly associated with two frontier MOs (HOMO and LUMO). In this case, the rates of optical excitation and de-excitation are determined by Eq. (5).

For the subsequent analysis we assume that the Coulomb interaction between excess electrons (or holes) occupying the molecule in the course of charge transfer, is so large that the molecule can only stay in its neutral ground (or excited) state, in its oxidized state and in its reduced state. These states are denoted as $M_0 = M(N_G)$, $M_* = M'(N_G), M_+ = M(N_G - 1)$ and $M_- = M(N_G + 1)$. Here, N_G is the number of electrons if the molecule is in its neutral state. If the maxima of electron location at the HOMO and LUMO are in the vicinity of the spaced sites I and II, cf. Fig. 1, one can suppose that the exchange interaction between the unpaired electrons occupying the HOMO and the LUMO becomes small. This allows one to ignore the exchange splitting between the singlet, $M_*(S)$ and triplet, $M_*(Tm), (m = 0, \pm 1)$ states of the excited molecule. Accordingly, the electron spin projections can be taken as good quantum numbers. Therefore, the fourfold degenerated excited state M_* can be characterized either by molecular spin states $(M_* = M_*(S), M_*(Tm))$ or by spin projections σ_H and σ_L of unpaired electrons occupying the frontier MOs $(M_* = M_*(\sigma_H, \sigma_L))$. At a negligible exchange interaction, both sets of spin quantum numbers lead to identical results. Moreover, the states $M_+ = M_+(\sigma_H)$ and $M_- = M_-(\sigma_L)$ are twofold degenerated.

To specify the energies $E_{M(N)}$ entering the molecular Hamiltonian (3) and the matrix elements in the interaction expression (4) we introduce the following notation of the Hamiltonian

$$H_m = \sum_j \sum_\sigma \left(\epsilon_j + U_j c^+_{j-\sigma} c_{j-\sigma} + \frac{1}{2} \sum_{j'(\neq j)} \sum_{\sigma'} U_{jj'} c^+_{j'\sigma'} c_{j'\sigma'} \right) c^+_{j\sigma} c_{j\sigma}, \tag{19}$$

and of the electron transfer coupling (cf. [48,52–54])

$$V_{tr} = \sum_j \sum_{r\mathbf{k}\sigma} \left(\beta_{jr\mathbf{k}} c^+_{j\sigma} a_{r\mathbf{k}\sigma} + \beta^*_{jr\mathbf{k}} a^+_{r\mathbf{k}\sigma} c_{j\sigma} \right). \tag{20}$$

In Eq. (19) the ϵ_j are the energies of an electron occupying the j(=H,L) th MO. The strength of the Coulomb interaction between two electrons is defined by U_j if both electrons occupy the jth MO. If the electrons belong to different MOs Coulomb interaction is measured by $U_{jj'}$. The operators $c^+_{j\sigma}$ and $c_{j\sigma}$ create or annihilate an electron in the molecule, and $\beta_{jr\mathbf{k}}$ characterizes the coupling of the jth MO to the $r\mathbf{k}$th band state of the electrode.

According to the Hamiltonian, Eq. (19), the molecular energies $E_{M(N)} = E_\alpha$, $(\alpha = 0, *, +, -)$ follow as:

$$\begin{aligned} &E_0 = 2\epsilon_H + U_H, \quad E_* = \epsilon_H + \epsilon_L + U_{LH}, \\ &E_- = 2\epsilon_H + \epsilon_L + U_H + 2U_{LH}, \quad E_+ = \epsilon_H. \end{aligned} \tag{21}$$

Here, ϵ_H and ϵ_L are the energies of an electron occupying the frontier MOs while U_H and U_{HL} are the Coulomb parameters. Concerning the matrix elements entering Eq. (4), all of them are expressed by the couplings $\beta_{Hr\mathbf{k}}$ or $\beta_{Lr\mathbf{k}}$. We have, for example, $\langle M_0 | V_{tr} | M_+(\sigma_H) r\mathbf{k}\sigma \rangle = \beta_{Hr\mathbf{k}} \delta_{-\sigma,\sigma_H}$ and $\langle M_0 r\mathbf{k}\sigma | V_{tr} | M_-(\sigma_L) \rangle = \beta^*_{Lr\mathbf{k}} \delta_{\sigma,\sigma_L}$.

3.1. Contact rate constants

Noting the structure of the transition matrix elements, the so-called wide band approximation [55] enables one to express the hopping transfer rates (10) and (11) by contact rate constants $K^{(r)}_{\alpha\alpha'}$. For instance, we get $\chi^{(r)}_{M_*(\sigma_H,\sigma'_L)\to M_-(\sigma_L)} = \delta_{\sigma'_L,\sigma_L} K^{(r)}_{*-}$. According to the used HOMO–LUMO model the forward contact rate constants takes the form

$$\begin{aligned} K^{(r)}_{0-} &\simeq (1/\hbar)\Gamma^{(r)}_L N(\Delta E_{-0}), \\ K^{(r)}_{*-} &\simeq (1/\hbar)\Gamma^{(r)}_H N(\Delta E_{-*}), \\ K^{(r)}_{+0} &\simeq (1/\hbar)\Gamma^{(r)}_H N(\Delta E_{0+}), \\ K^{(r)}_{+*} &\simeq (1/\hbar)\Gamma^{(r)}_L N(\Delta E_{*+}). \end{aligned} \tag{22}$$

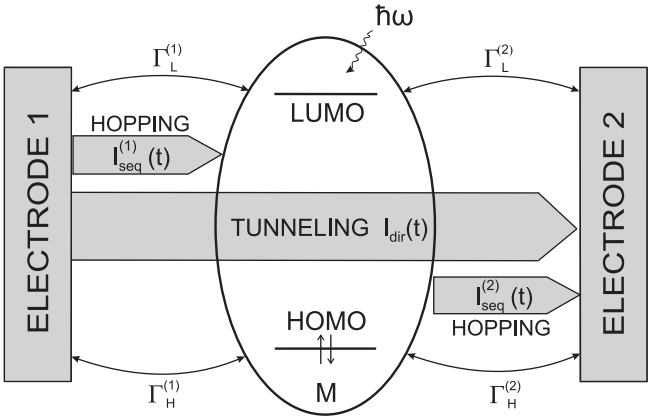

Fig. 2. HOMO–LUMO scheme related to the electron transfer through the **1**-M-**2** molecular junction. The width parameters $\Gamma^{(r)}_j$ characterize the efficiency of contact electron jumps as well as of the direct (tunneling) electron transfer. The sequential current components $I^{(1)}_{seq}(t)$ and $I^{(2)}_{seq}(t)$ can differ from each other if the junction is transient regime.

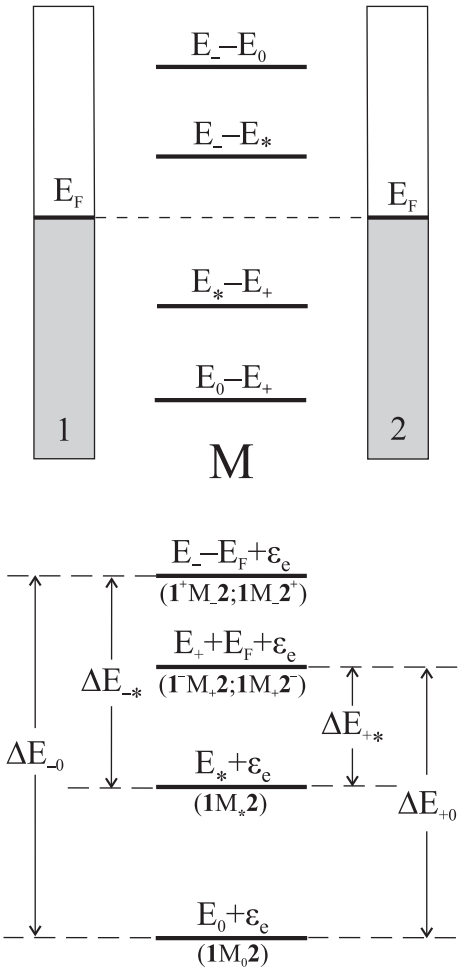

Fig. 3. Charging energies $E_0 - E_+, E_* - E_+, E_- - E_+$ and $E_- - E_*$ (upper panel) and transmission gaps related to the charged molecular states M_+ and M_- (lower panel).

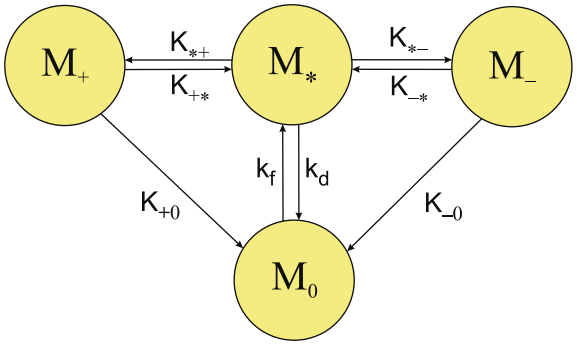

Fig. 4. Kinetic scheme of the transfer processes occurring in the molecular junction in the absence of an applied voltage (for further details see text).

The quantities

$$\Gamma_j^{(r)} \simeq 2\pi \sum_{\mathbf{k}} |\beta_{j r\mathbf{k}}|^2 \delta(E - E_{r\mathbf{k}}) \tag{23}$$

characterize electron hopping between the jth MO and the rth electrode (cf. Fig. 2), whereas the distribution function

$$N(\Delta E_{\alpha'\alpha}) = \left[\exp(\Delta E_{\alpha'\alpha}^{(r)}/k_B T) + 1\right]^{-1}. \tag{24}$$

determines the influence of temperature on the hopping processes via the transmission gaps

$$\Delta E_{+0(*)} = (E_+ + E_F) - E_{0(*)} \tag{25}$$

and

$$\Delta E_{-0(*)} = E_- - (E_{0(*)} + E_F). \tag{26}$$

Backward contact rate constants which characterize the transition of an electron from the molecule to the rth electrode are connected with the forward ones, Eq. (22), by the relation

$$K_{\alpha\alpha'}^{(r)} = K_{\alpha'}^{(r)} \alpha \exp(-\Delta E_{\alpha'\alpha}/k_B T). \tag{27}$$

The physical meaning of the transmission gaps can be easily deduced from their definition. Since $E_- - E_0$ and $E_+ - E_0$ are the electron charging and electron discharging energies (with respect to the molecule being in its ground neutral state), respectively, the inequalities $E_- - E_0 > E_F$ and $E_0 - E_+ < E_F$ have to be fulfilled in the unbiased **1**-M-**2** system with identical electrodes (cf. the upper panel in Fig. 3 where $\mu_1 = \mu_2 = E_F$). Therefore, the gaps ΔE_{-0} and ΔE_{+0} are both positive. When the molecule is in the excited state, then respective charging and discharging energies, $E_- - E_*$ and $E_+ - E_*$, can be higher or lower than the Fermi level and, thus, transmission gaps ΔE_{-*} and ΔE_{+*} can become positive or negative. [One possible case with $E_- - E_* > E_F$ and $E_* - E_+ < E_F$, is presented at the upper panel in Fig. 3.]

An additional interpretation of the transmission gaps follows from a comparison of electron energies belonging the whole **1**-M-**2** system [38,39]. Let $\mathcal{E}_e$ be the energy of electrons in the electrodes. In the case of a neutral molecule the energy of the whole system is $E(\mathbf{1}M_{0(*)}\mathbf{2}) = E_{0(*)} + \mathcal{E}_e$. During a charge transmission process the number of electrons in the system is conserved. Therefore, the energies of the system with the oxidized and reduced molecule are, respectively, $E(\mathbf{1}^- M_+ \mathbf{2}) = E(\mathbf{1}M_+\mathbf{2}^-) = E_+ + \mathcal{E}_e + E_F$ and $E(\mathbf{1}^+ M_- \mathbf{2}) = E(\mathbf{1}M_-\mathbf{2}^+) = E_- + \mathcal{E}_e - E_F$. Therefore, the gaps (25) and (26) correspond to the difference between the above noted energies, i.e. $\Delta E_{+0(*)} = E(\mathbf{1}^- M_+ \mathbf{2}) - E(\mathbf{1}M_{0(*)}\mathbf{2}) = E(\mathbf{1}M_+\mathbf{2}^-) - E(\mathbf{1}M_{0(*)}\mathbf{2})$ and $\Delta E_{-0(*)} = E(\mathbf{1}^+ M_- \mathbf{2}) - E(\mathbf{1}M_{0(*)}\mathbf{2}) = E(\mathbf{1}M_-\mathbf{2}^+) - E(\mathbf{1}M_{0(*)}\mathbf{2})$ (cf. Fig. 3 lower panel). Such interpretation of the transmission gaps is quite suitable for the analysis of the transmission processes in the molecular junctions.

The sign of the transmission gap defines the electron transfer along a given transmission channel. For instance, if ΔE_{+*} is positive, then the transition $M_+ \to M_*$ caused by an electron injected into the molecule, requires a thermal activation i.e. it proceeds in an off-resonant regime. If $\Delta E_{+*} < 0$, however, the $M_+ \to M_*$ transition does not require any thermal activation and, thus, becomes practically independent on the absolute value of ΔE_{+*}. Consequently, the electron hopping takes place in a resonant regime.

3.2. Inelastic tunnel rate constant

Eq. (14) for the direct (tunnel) transfer rate indicates that in the absence of an applied voltage any elastic electron tunneling between identical electrodes disappears. We study in the following an inelastic tunneling event which is accompanied by the intramolecular transition $M_* \to M_0$. To derive a respective rate expression we first consider the effect of the molecule–electrode coupling. Since it is not too strong, its presence may be accounted for by a shift $\Delta E_{M(N)}$ of the molecular energies as well as by a level broadening

$$\Gamma_{M(N)}/2 = \pi \sum_r \sum_{M'} \sum_{\mathbf{k}\sigma} \Big\{ |V_{M(N) r\mathbf{k}\sigma; M'(N+1)}|^2 \times \delta[E_{M'(N+1)} - E_{M(N)} - E_{r\mathbf{k}}] + |V_{M(N); M'(N-1) r\mathbf{k}\sigma}|^2 \delta[E_{M(N)} - E_{M'(N-1)} - E_{r\mathbf{k}}] \Big\}. \tag{28}$$

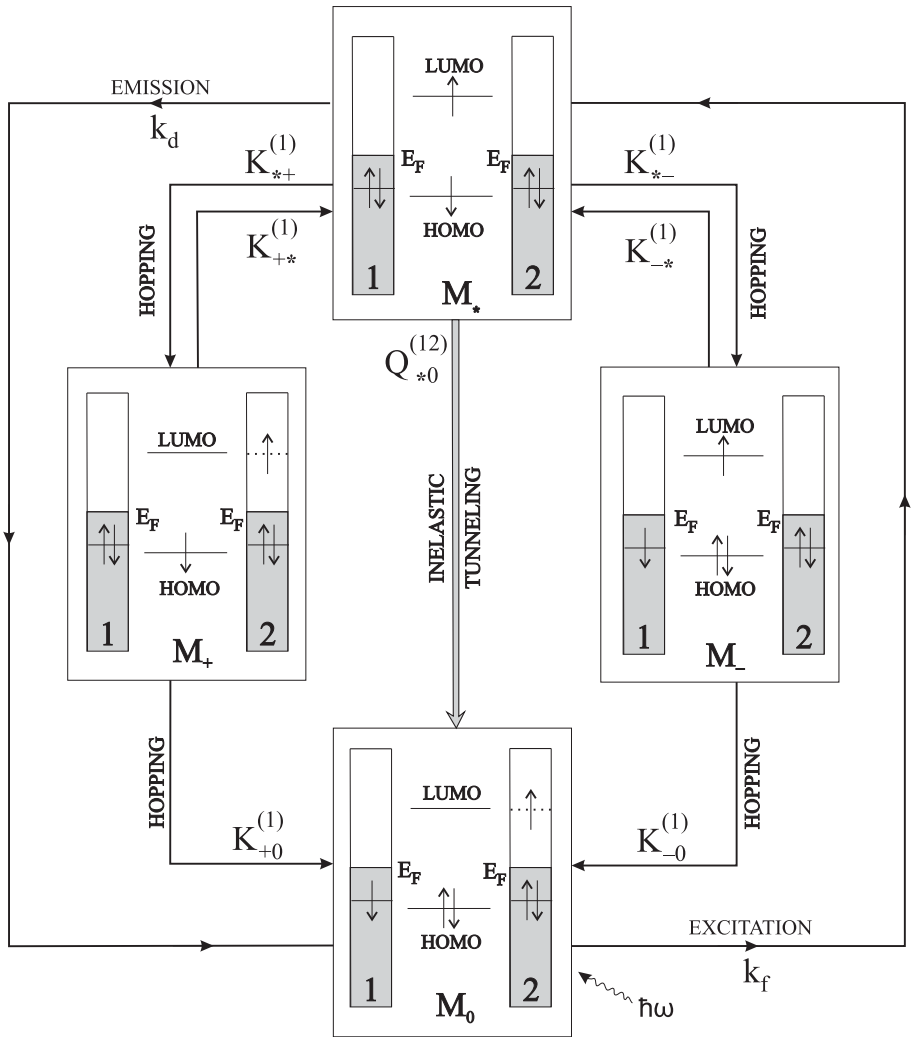

Fig. 5. Transfer routes of the light-induced interelectrode $\mathbf{12} \rightarrow \mathbf{1}^{+}\mathbf{2}^{-}$ electron transmission including the participation of the charged molecular states M_{+} and M_{-}. Within the transmission along the sequential route, the charged states are populated while the same states participate in a virtual form only if the transfer proceeds along the tunnel route.

Accordingly, the Green's operator, determining the general transition amplitude is defined by these shifted and broadened molecular energies. Due to the weak molecule–electrode coupling one can omit the energy shift $\Delta E_{M(N)}$. Taking the Hamiltonian, Eq. (19), then, in the framework of the HOMO–LUMO model, the unperturbed molecular energies, Eq. (21) are expressed via the single-electron energies ϵ_H and ϵ_L as well as via the Coulomb parameters U_H and U_{LH}. The broadenings, Eq. (28) are defined by the single-electron level broadenings $\Gamma_j/2$. The quantities

$$\Gamma_j = \sum_r \Gamma_j^{(r)}, \quad (j = H, L), \tag{29}$$

are obtained as the sum of the width parameters $\Gamma_j^{(r)}$, Eq. (23). Thus, the described formulation of the Green's operator $\widehat{G}(E)$ and the introduction of the width parameters results in the following rate expression

$$Q_{rM_*(\sigma_L,\sigma_H)\rightarrow r'M_0} = Q_{*0}^{(rr')} \simeq \frac{1}{\pi\hbar}\left[\frac{\Gamma_L^{(r')}\Gamma_H^{(r)}}{\Gamma_+}\left(\varphi_{+\rightarrow 0} - \varphi_{+\rightarrow *}\right) + \frac{\Gamma_L^{(r')}\Gamma_H^{(r)}}{\Gamma_-} \times \left(\varphi_{-\rightarrow 0} - \varphi_{-\rightarrow *}\right)\right]. \tag{30}$$

Here we used $\Gamma_+ = \sum_r(\Gamma_H^{(r)} + 2\Gamma_L^{(r)})$ and $\Gamma_- = \sum_r(\Gamma_L^{(r)} + 2\Gamma_H^{(r)})$. According to Eq. (30) the regime of inelastic tunneling transfer is governed by the quantities

$$\varphi_{\alpha'\rightarrow\alpha} = \text{arc tn}(2\Delta E_{\alpha'\alpha}/\Gamma_{\alpha'}). \tag{31}$$

For the weak molecule–electrode coupling under consideration the width parameters do not exceed 10^{-3} eV. Accordingly, we have $|\Delta E_{\alpha'\alpha}/\Gamma_{\alpha'}| \gg 1$, and one can use the asymptotic form $\varphi_{\alpha'\rightarrow\alpha} \approx (\pi/2)(\text{sign}\Delta E_{\alpha'\alpha}) - (\Gamma_{\alpha'}/2\Delta E_{\alpha'\alpha})$. It follows the particular relation $\varphi_{+\rightarrow 0} - \varphi_{+\rightarrow *} \approx (\pi/2)(1 - \text{sign}\Delta E_{+*}) + [(\Gamma_+/2\Delta E_{+*}) - (\Gamma_+/2\Delta E_{+0})] \approx (\pi/2)[(1 - \text{sign}\Delta E_{+*}) + (\Gamma_+/\pi\Delta E_{+*})]$. Taking $\Delta E_{+*} > 0$ then $\varphi_{+\rightarrow 0} - \varphi_{+\rightarrow *} \approx (\Gamma_+/\pi\Delta E_{+*}) \ll 1$. In the contrary case $\Delta E_{+*} < 0$ we find $\varphi_{+\rightarrow 0} - \varphi_{+\rightarrow *} \approx \pi$ what is much larger then the respective expression deduced for $\Delta E_{+*} > 0$. Note also that at the resonant regime of tunnel electron transmission the $\varphi_{+\rightarrow 0} - \varphi_{+\rightarrow *}$ is independent of the actual value of the transmission gap.

3.3. Rate equations for integral molecular populations

The kinetics in the junction are dominated by sequential processes which are characterized by contact rate constants $K_{\alpha\alpha'}^{(r)}$. But, the direct inelastic electron tunneling responsible for the

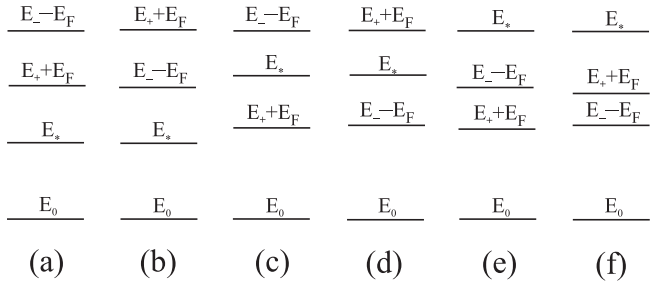

Fig. 6. Feasible energy levels of the molecular junctions in the absence of an applied voltage. E_0, E_*, E_+ and E_- are the molecular energies and E_F denotes the electrode Fermi energy.

Table 1
Parameters of the HOMO–LUMO model ($\Delta E_{\pm *}$ and $\Gamma_j^{(i)}$ are given in eV).

Figures	ΔE_{+*}	ΔE_{-*}	$\Gamma_L^{(1)}$	$\Gamma_L^{(2)}$	$\Gamma_H^{(1)}$	$\Gamma_H^{(2)}$	T, K
7	0.4	0.8	10^{-6}	10^{-4}	10^{-5}	10^{-6}	300
8	0.1	0.8	10^{-6}	10^{-4}	10^{-5}	10^{-6}	300
9	0.1	0.8	10^{-6}	10^{-4}	10^{-5}	10^{-6}	100
10	−0.1	0.8	10^{-7}	10^{-5}	10^{-6}	10^{-7}	300
11	0.8	−0.1	10^{-7}	10^{-5}	10^{-6}	10^{-7}	300
12	−0.1	−0.2	10^{-7}	10^{-5}	10^{-6}	10^{-7}	300

transitions between the excited and the ground states of the neutral molecule, is also important. For instance, the distant rate constants $Q_{*0}^{(rr')}$ describe the nonradiative decay of the excited molecule. The kinetic scheme depicted in Fig. 4 illustrates the possible transition processes in the junction including the *cw*-optical excitation of the molecule. All rates indicated in Fig. 4 characterize the transitions with the participation of the degenerated molecular states M_*, M_+ and M_-. Therefore, it is convenient to introduce integral molecular populations

$$\begin{aligned} P(*;t) &= \sum_{\sigma_H,\sigma_L} P(M_*(\sigma_H,\sigma_L);t), \\ P(+;t) &= \sum_{\sigma_H} P(M_+(\sigma_H);t), \\ P(-;t) &= \sum_{\sigma_L} P(M_-(\sigma_L);t), \end{aligned} \tag{32}$$

[note also that $P(*;t) = P_*(S;t) + \sum_{m=0,\pm1} P_*(Tm);t)$]. The quantities introduced in Eq. (32) along with the population $P(0;t) \equiv P(M_0;t)$ obey the normalization condition

$$\sum_{\alpha=0,*,+,-} P(\alpha;t) = 1, \tag{33}$$

which corresponds to Eq. (15). Based on the introduction of integral populations, the general kinetic equation (16) reduce to the following set of rate equations

$$\begin{aligned} \dot{P}(0;t) &= -k_f P(0;t) + K_{+0}P(+;t) + K_{-0}P(-;t) + k_d P(*;t), \\ \dot{P}(+;t) &= -(K_{+0} + 2K_{+*})P(+;t) + K_{*+}P(*;t), \\ \dot{P}(-;t) &= -(K_{-0} + 2K_{-*})P(-;t) + K_{*-}P_*(t), \\ \dot{P}(*;t) &= -(K_{*+} + K_{*-} + k_d)P(*;t) + 2K_{+*}P(+;t) + 2K_{-*}P(-;t) + k_f P_0(t). \end{aligned} \tag{34}$$

Here, we introduced the recharge transfer rates

$$K_{\alpha\alpha'} = K_{\alpha\alpha'}^{(1)} + K_{\alpha\alpha'}^{(2)}, \tag{35}$$

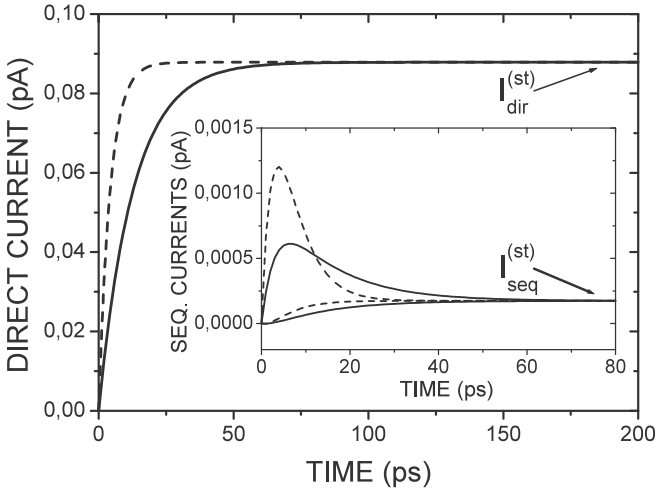

Fig. 7. Transient current components for an off-resonant charge transmission process and at a different intensities of optical excitation. Solid lines: $k_f = 10^{10}\ s^{-1}$, dashed lines: $k_f = 3 \cdot 10^{10}\ s^{-1}$. Insert: sequential current components $I_{seq}^{(1)}(t)$ (upper curves) and $I_{seq}^{(2)}(t)$ (lower curves) approach the common steady state value.

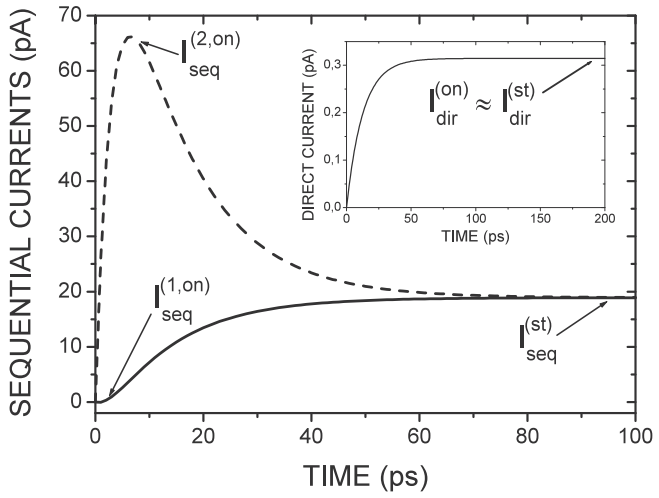

Fig. 8. Off-resonant regime of current formation at a small transmission gap ΔE_{+*}.

which are expressed by the sum of contact rate constants. The rate constant $k_f = K_{0*}^{(f)}$, Eq. (18) characterizes the optical transition between molecular singlet states $M(N) = M_0$ and $M'(N) = M_*(S)$. Accordingly, the overall decay rate from the fourfold degenerated excited state follows as

$$k_d = k_f/4 + Q_{*0}. \tag{36}$$

We defined

$$Q_{*0} = Q_{*0}^{(12)} + Q_{*0}^{(21)} \tag{37}$$

as the component caused by the coupling of the molecule to the electrodes. The concrete expression for Q_{*0} can be deduced from Eq. (30). It reads

$$Q_{*0} \simeq \frac{1}{2\hbar}\left(\Gamma_H^{(1)}\Gamma_L^{(2)} + \Gamma_H^{(2)}\Gamma_L^{(1)}\right)R \tag{38}$$

with

$$\begin{aligned} R = \Gamma_+^{-1}[(1 - \mathrm{sign}\Delta E_{+*}) + (\Gamma_+/\pi\Delta E_{+*})] + \Gamma_-^{-1}[(1 - \mathrm{sign}\Delta E_{-*}) \\ + (\Gamma_-/\pi\Delta E_{-*})]. \end{aligned} \tag{39}$$

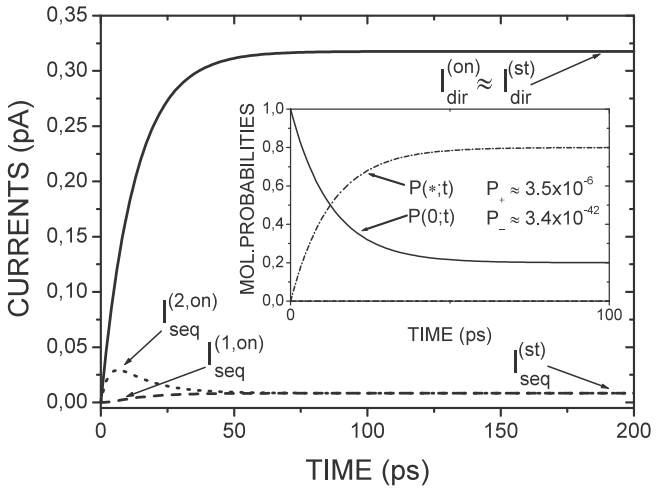

Fig. 9. Off-resonant current formation at low temperature with the participation of the charged molecular state M_+.

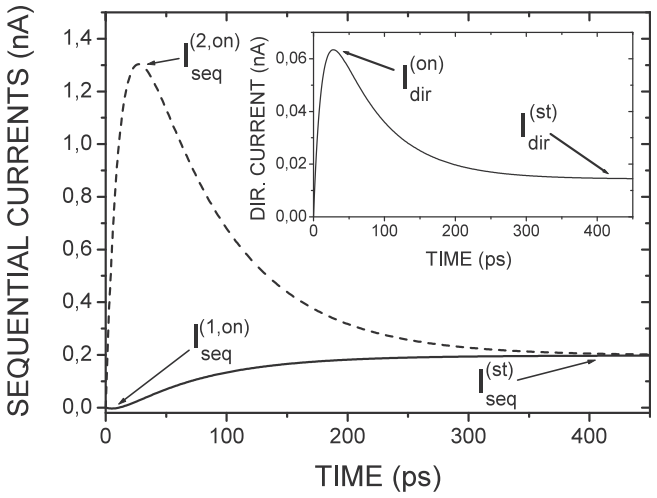

Fig. 10. Single-channel resonant charge transmission with the participation of the charged molecular state M_+ (the energy gap ΔE_{+*} is negative). The total current is mainly determined by the sequential components.

4. The Photocurrent

Already in the absence of an applied voltage a photocurrent, Eq. (8) has to be expected. According to the used HOMO–LUMO model and by noting the Eqs. (10), (11), (22) and (27) for the sequential current component, Eq. (9), we find

$$I^{(r)}_{seq}(t) = (\delta_{r,1} - \delta_{r,2}) I_0 \pi\hbar \Big\{ \Big[K^{(r)}_{*-} P(*;t) + \Big(K^{(r)}_{+0} + 2K^{(r)}_{+*} \Big) P(+;t) \Big] - \Big[K^{(r)}_{*+} P(*;t) + \Big(K^{(r)}_{-0} + 2K^{(r)}_{-*} \Big) P(-;t) \Big] \Big\}, \tag{40}$$

where $I_0 = |e|/\pi\hbar \times 1\text{eV} \approx 77.6\ \mu\text{A}$ is the current unit [56]. It follows from Eq. (40) that the charge transmission along the sequential route is determined by hopping (contact) rate constants (22) and (27). The time-dependent behavior of this current component is determined by the molecular state populations $P(+;t), P(-;t)$ and $P(*;t)$. The direct component of the current is formed by the inelastic tunnel electron transmission along the channel related to the excited molecule. The expression for the direct component follows from Eqs. (12), (13), and (30) and takes the form

$$I_{dir}(t) = I_0 \pi\hbar S_{*0} P(*;t). \tag{41}$$

Here, we introduced

$$S_{*0} = Q^{(12)}_{*0} - Q^{(21)}_{*0} \simeq \frac{1}{2\hbar} \Big(\Gamma^{(1)}_H \Gamma^{(2)}_L - \Gamma^{(2)}_H \Gamma^{(1)}_L \Big) R, \tag{42}$$

what represents the net tunnel electron flow (R has been introduced in Eq. (39)). Eqs. (41) and (42) show that, the sign of the direct current component (in the HOMO–LUMO model) is determined by the sign of $\Gamma^{(1)}_H \Gamma^{(2)}_L - \Gamma^{(2)}_H \Gamma^{(1)}_L$. Moreover, the time-dependent behavior of the direct current component is determined by the population $P(*;t)$.

The scheme of the electron transfer routes, as displayed in Fig. 5, offers the opportunity to analyze further details of the current formation. Charge transitions are represented by $\mathbf{12} \to \mathbf{1}^+\mathbf{2}^-$. According to Fig. 5 a possible current formation results from the decay of the excited molecular state. This is possible via the sequential route (including the formation of the charged molecular states M_+ and M_-) as well as via the direct route $M_* \to M_0$. Both routes include two (left and right) transmission channels. The left sequential channel, $\mathbf{1}M_*\mathbf{2} \rightleftarrows \mathbf{1}M_+\mathbf{2}^- \to \mathbf{1}^+M_0\mathbf{2}^-$, proceeds across the charged molecular state M_+. This state is formed by an electron hopping from the LUMO to the electrode 2 (with contact rate constant $K^{(2)}_{*+}$) after which another electron hops from the electrode 1 to the HOMO (with contact rate constant $K^{(1)}_{+0}$). In summary, we have the transition $\mathbf{12} \to \mathbf{1}^+\mathbf{2}^-$. This transition is also achieved by an electron transmission along the right sequential channel $\mathbf{1}M_*\mathbf{2} \rightleftarrows \mathbf{1}^+M_-\mathbf{2} \to \mathbf{1}^+M_0\mathbf{2}^-$ which includes the charged molecular state M_-. The M_- state is formed by an electron hopping from electrode 1 to the HOMO. The transfer of an electron from the LUMO to electrode 2 returns the molecule to its neutral ground state M_0. The respective sequential charge transfer steps are characterized by the contact hopping rates $K^{(1)}_{*-}$ and $K^{(2)}_{-0}$. It is important to underline that during the electron transmission along the sequential route, the current formation is accompanied by a molecular recharging, i.e. by a population of the intermediate charged molecular states M_+ and M_-.

The second type of transfer route shown Fig. 5, refers to the direct (distant) interelectrode electron transfer $\mathbf{12} \to \mathbf{1}^+\mathbf{2}^-$ which is accompanied by the $M_* \to M_0$ transition in the molecule. In contrast to the sequential route, electron transmission along the direct route $\mathbf{1}M_*\mathbf{2} \to \mathbf{1}^+M_0\mathbf{2}^-$ does not result in a change of the charged molecular states populations (these states only participate as virtual states). Thus, a direct electron transfer constitutes an inelastic tunneling event of an electron between the electrodes. The related distant transfer rate $Q^{(12)}_{*0}$ is defined in Eq. (30). Since a reverse route $\mathbf{1}M_0\mathbf{2} \leftarrow \mathbf{1}^-M_*\mathbf{2}^+$ is formed in a similar way and is characterized by the rate $Q^{(21)}_{*0}$, the direct current component is proportional to the net electron flow S_{*0}, Eq. (42).

5. Results and discussion

The Eqs. (8), (40), and (41) allow one to describe the time-dependent evolution of the photocurrent in the molecular junction starting with the switch-on of a *cw*-optical excitation (at $t = 0$) and extending up to the formation of a steady-state current $I_{st} = I_1(t \gg \tau_{st}) = I_2(t \gg \tau_{st})$ where τ_{st} is the characteristic time of the steady state formation. The kinetic schemes drawn in the Figs. 4 and 5 show that a control of the light-induced electron transfer is achieved via the transitions between electronic states M_0, M_*, M_+ and M_- of the molecule. Here, the charged molecular states M_+ and M_- are of particular importance since those participate in the transmission channels formation related to the sequential and the direct electron transfer routes. As far as the charged states population is determined by the relation between forward and backward contact rate constants, Eqs. (22) and (27), the position

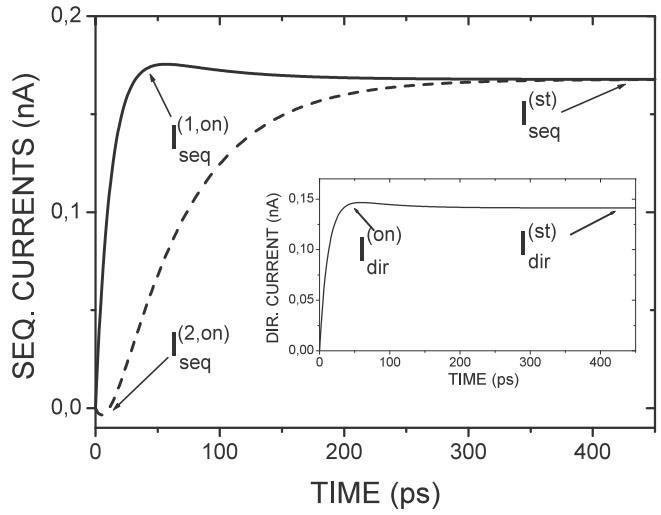

Fig. 11. Single-channel resonant transmission with the participation of the charged molecular state M_-.

of the energy levels in the **1**-M-**2** system predetermines the specific form of the interelectrode $\mathbf{12} \rightarrow \mathbf{1}^+\mathbf{2}^-$ and $\mathbf{1}^-\mathbf{2}^+ \leftarrow \mathbf{12}$ electron transmission.

Possible arrangements of the molecular junctions energy levels are depicted in Fig. 6. For the sake of simplicity, the electron energy $\mathcal{E}_e$ of the electrodes is omitted (cf. Fig. 3, lower panel where this energy is presented). If the junction energy with the neutral molecule in its excited state is below the energy valid if the molecule is in a charged state, then only an off-resonant regime of light-induced electron transmission becomes possible (cases (a) and (b)). The cases (c) and (d) correspond to charge transmission with a single resonant channel (either the oxidized or the reduced molecule is involved). Two further transmission channels are realized if the junction energy with the neutral molecule in its excited state exceeds the energies realized for the oxidized or the reduced molecule (cases (e) and (f)).

The further analysis will be based on the Eqs. (8), (40), (41) for the current as well as the Eqs. (22) and (27) defining the contact rate constants. Additionally, the expressions (37)–(39) for the tunnel decay rate Q_{*0} and Eq. (42) for net electron flow S_{*0} are taken into account. The time-dependent evolution of the integral molecular populations $P(\alpha;t)$ are determined by the rate Eqs. (34) where the recharge rate constants are given by Eq. (35). Initial conditions for the populations are found from a solution of the rate Eqs. (34) if one sets $\dot{P}(\alpha;t)=0$ and $k_f=0$. Since the relations $K_{0-}\simeq 0$ and $K_{0+}\simeq 0$ are valid for the case of a charge transmission in the absence of an applied voltage, it follows $P(*;0)\simeq 0$, $P(+;0)\simeq 0, P(-;0)\simeq 0$ and $P(0;0)\simeq 1$. As already indicated the hopping and the tunnel transition processes can proceed in off-resonant or a resonant regime depending on the sign of the actual transmission gap, cf. Eqs. (25) and (26).

Although the calculations have been performed on the basis of the general expressions (34), and (40)–(42), including Eqs. (30), (31), (36)–(39), most of the findings will be discussed in terms of analytical expressions. Those are derived for cases where an electron transfer occurs preliminary along a separate transmission channel. For the sake of definiteness, we consider a charge transmission process where the energy $E_- - E_F$ is larger than E_* and $E_+ + E_F$ (see the cases (a) and (c) in Fig. 6). We also suppose that ΔE_{-*} is large enough to neglect the population of the state M_-. This means that the off-resonant and resonant regimes of light-induced current formation involve an electron transfer process predominantly across the three molecular states, M_0, M_* and M_+ (the left route in Fig. 5). Thus, charge transmission only occurs along the channel related to the charged molecular state M_+. To achieve an analytic description of this transmission process one has to set $K_{*-}\simeq 0$. This leads to the following solution of the Eq. (34):

$$
\begin{aligned}
&P(0;t)\simeq P_0+\frac{k_f}{k_1k_2(k_1-k_2)}\times\left[k_2(k_1-\lambda_+-K_{*+})e^{-k_1t}-k_1(k_2-\lambda_+-K_{*+})e^{-k_2t}\right],\\
&P(*;t)\simeq P_*+\frac{k_f}{k_1k_2(k_1-k_2)}\left[-k_2(k_1-\lambda_+)e^{-k_1t}+k_1(k_2-\lambda_+)e^{-k_2t}\right],\\
&P(+;t)\simeq P_+ +\frac{k_fK_{*+}}{k_1k_2(k_1-k_2)}\left[k_2e^{-k_1t}-k_1e^{-k_2t}\right],\\
&P(-;t)\simeq 0.
\end{aligned}
\tag{43}
$$

The quantities

$$
\begin{aligned}
&P_0=(K_{*+}K_{+0}+k_d\lambda_+)/k_1k_2,\\
&P_+=k_fK_{*+}/k_1k_2,\quad P_-=0,\\
&P_*=k_f\lambda_+/k_1k_2
\end{aligned}
\tag{44}
$$

are steady state populations and the overall transfer rates take the form

$$
k_{1,2}=(1/2)\left[a\pm\sqrt{a^2-4b^2}\right].
\tag{45}
$$

Note the abbreviations $a=k_f+\lambda_++\lambda_*, b^2=k_f(\lambda_++K_{*+})+\lambda_*K_{+0}+2k_dK_{+*}$, and $\lambda_+\equiv K_{+0}+2K_{+*}, \lambda_*\equiv K_{*+}+k_d$, Based on the Eqs. (40)–(43) one can derive analytic expressions for the sequential and direct current components. The time evolution of these components is determined by the overall transfer rates k_1 and k_2. Obviously, the formation of a finite photocurrent in the absence of an applied voltage only becomes possible at an *asymmetric* coupling of the molecule to the electrodes. As it was already noted such asymmetry can result from nonidentical electron density at the HOMO and the LUMO (cf. Fig. 1). For the following we assume $\Gamma_H^{(1)}>\Gamma_H^{(2)}$, $\Gamma_L^{(2)}>\Gamma_L^{(1)}$. Since the factor $\Gamma_H^{(1)}\Gamma_L^{(2)}-\Gamma_H^{(2)}\Gamma_L^{(1)}$ becomes positive the steady state electron current is also a positive (electrons move from electrode 1 to electrode 2).

Next let us consider the current formation at a weak molecule–electrode coupling (when the width parameters are of the order $(10^{-7}-10^{-4})$ eV) and at a moderate optical excitation

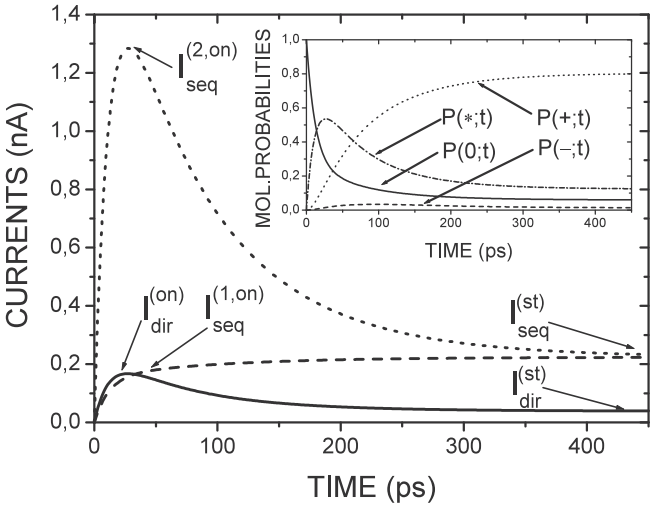

Fig. 12. Two-channel resonant charge transmission. There is no basic difference between the behavior of the current components formed by a single-channel of charge transmission (except a certain increase of the direct component, cf. also Fig. 10). The evolution of the current components follow the time-dependent behavior of the molecular probabilities (see insert).

($k_f = 10^{10}$ s^{-1}). The excitation energy is $\hbar\omega = E_* - E_0 = 1.6$ eV. The various parameters are collected in Table 1.

5.1. Off-resonant regime of charge transmission

Figs. 7–9 demonstrate the transient behavior of the direct and sequential current components for a positive transmission gap ΔE_{+*} (it determines the efficiency of the $M_* \to M_+$ transition due to thermal activation).

5.1.1. Deep off-resonant regime

In the case represented in Fig. 7, the gap ΔE_{+*} is assumed to be a rather large so that the population of the charged molecular state M_+ is small. As a result, charge transmission mainly follows the tunneling route whereas thermal activation of the molecular state M_+ (as well as state M_-) is suppressed (cases (a) and (b) of Fig. 6). For such a transmission the distant current component strongly exceeds the sequential one (see the insert). Therefore, the total current, Eq. (8) is associated with the direct component:

$$I_r(t) \simeq I_{dir}(t) \simeq I_{dir}^{(st)}\left(1 - e^{-t/\tau_{st}}\right). \tag{46}$$

Here, $\tau_{st} = k_{st}^{-1} = (k_f + k_d)^{-1}$ is the characteristic time of the evolution of the current to its steady state value

$$I_{dir}^{(st)} = I_0 \pi \hbar S_{*0}(k_f/k_{st}). \tag{47}$$

The quantities S_{*0} and Q_{*0} (the latter enters k_d, cf. Eq. (36)) have been defined in the Eq. (38) and Eq. (42), respectively, additionally using $R \simeq (1/\pi)[(\Delta E_{+*})^{-1} + (\Delta E_{-*})^{-1}]$.

In the off-resonant regime, the inequality $k_f \gg Q_{*0}$ is valid with a good accuracy. As a result, a dependence of the photocurrent on the light intensity (i.e. on the rate k_f) is only present within the transient behavior whereas the steady state value, $I_{st} = I_{dir}^{(st)}$, becomes independent on k_f (see Fig. 7). We also note that the single-exponential kinetics correctly describes the transfer process until the population of the charged molecular state M_+ (and M_-) becomes so small that the direct current component strongly exceeds the sequential one.

5.1.2. Single-channel off-resonant regime

The Figs. 8–10 depict how the current components approach their steady-state values for the case of a large and positive gap ΔE_{-*} and a positive but not so large gap ΔE_{+*}. Here, an activation of the hopping process $M_* \to M_+$ is possible and the contribution of the sequential component to the total one becomes significant. As a result, the transient behavior of the current represents two-exponential kinetics. For instance, a comparison of Figs. 7 and 8 shows that at a small gap ΔE_{+*} (but at the same width parameters and temperature), an electron transmission along the sequential route becomes more effective than the transmission along the tunnel route. Therefore, the total current is not caused by the direct component (as in Fig. 7) but by the sequential one (cf. Fig. 8). As a result, the total currents $I_1(t) \simeq I_{seq}^{(1)}(t)$ and $I_2(t) \simeq I_{seq}^{(2)}(t)$ do not coincide in the transient region. Such a behavior is originated by an asymmetric hopping of electrons between the molecule and the electrodes. A temperature decrease does not predominantly impact the direct component but strongly reduces the sequential one, as deduced from a comparison of Figs. 9 and 8.

For a further inspection of the transient current either in the off-resonant or the resonant regime we use analytic expressions which follow from the Eqs. (40), (41) and (43). Let us start with an analysis of the sequential current components

$$I_{seq}^{(r)}(t) = I_{seq}^{(st)}\left[1 - \frac{1}{k_1 - k_2}\left(k_1 e^{-k_2 t} - k_2 e^{-k_1 t}\right)\right] + (-1)^r I_0 \pi \frac{k_f \Gamma_L^{(r)}}{k_1 - k_2} N(\Delta E_{+*})\left(e^{-k_2 t} - e^{-k_1 t}\right), \tag{48}$$

where the quantity

$$I_{seq}^{(st)} = I_0 \pi \frac{k_f}{\hbar k_1 k_2}(\Gamma_H^{(1)}\Gamma_L^{(2)} - \Gamma_H^{(2)}\Gamma_L^{(1)})N(\Delta E_{+*}) \tag{49}$$

denotes the steady state sequential current entering $I_{seq}^{(1)}(t)$ and $I_{seq}^{(2)}(t)$.

The results depicted in the Figs. 8 and 9 refer to an electrode–molecule coupling which guarantees $k_1 \gg k_2$ where $k_1 \simeq k_f + k_d$ and $k_2 \simeq (1/\hbar)[\Gamma_L(2 - N(\Delta E_{+*})) + \Gamma_H]$. Due to the inequality $k_1 \gg k_2$ the fast and the slow kinetic periods of the time evolution are well determined. This allows one to distinguish between the currents $I_{seq}^{(1)}(t)$ and $I_{seq}^{(2)}(t)$. The fast kinetic phase covers a time region of the order of k_1^{-1} and starts just after the switching on of the optical excitation. The phase ends at $t \gtrsim 5k_1^{-1}$ from which the time-dependent behavior of the current is determined by the slow phase

$$I_{seq}^{(r)}(t) \simeq I_{seq}^{(st)}\left(1 - e^{-t/\tau_{st}}\right) + I_{seq}^{(r,on)} e^{-t/\tau_{st}}. \tag{50}$$

Here, $\tau_{st} = k_2^{-1}$ is the characteristic time the current needs to achieve its steady state value. The expression

$$I_{seq}^{(r,on)} = (-1)^r I_0 \pi \Gamma_L^{(r)} N(\Delta E_{+*}) \tag{51}$$

gives the current component valid at $t \ll \tau_{st}$. The sign of the $I_{seq}^{(r,on)}$ is determined by the direction of electron motion from the photoexcited molecule to the rth electrode. Since in the case under consideration, the transmission channel is associated with the charged molecular state M_+, the $M_* \to M_+$ transition involves an electron which leaves the LUMO and is captured by either the 1st or the 2nd electrode. In the scheme depicted in Fig. 5 this transition is accompanied by an electron hopping from the LUMO to electrode 1 and is characterized by the contact rate constant $K_{*+}^{(1)}$.

As a quantifier of the transient kinetics we introduce the ratio

$$\eta_{seq}^{(r)} = \left|I_{seq}^{(r,on)}\right| \Big/ I_{seq}^{(st)}. \tag{52}$$

It indicates how strongly the sequential components differ from their steady state value if the optical excitation is switched on. Our studies show that the difference between these quantities can become large if the difference between the width parameters is large. We illustrate this observation for the case $\Gamma_H^{(1)} \gg \Gamma_H^{(2)}$ and $\Gamma_L^{(2)} \gg \Gamma_L^{(1)}$ so that $\Gamma_H^{(1)}\Gamma_L^{(2)} - \Gamma_H^{(2)}\Gamma_L^{(1)} \approx \Gamma_H^{(1)}\Gamma_L^{(2)}$. Therefore, if, for instance, $\Gamma_H^{(1)} = 0.1\Gamma_L^{(2)}$ then $\eta^{(r)} \simeq (\Gamma_L^{(r)}/\Gamma_H^{(1)})(2 - N(\Delta E_{+*}))$ and thus $|I_{seq}^{(1,on)}| \ll I_{seq}^{(st)}$ whereas $I_{seq}^{(2,on)} \gg I_{seq}^{(st)}$, cf. Fig. 8.

During the slow kinetic phase the behavior of the direct current component is described by the expression

$$I_{dir}(t) \simeq I_{dir}^{(st)}\left(1 - e^{-t/\tau_{st}}\right) + I_{dir}^{(on)} e^{-t/\tau_{st}}. \tag{53}$$

The two current components,

$$I_{dir}^{(st)} = I_0 \pi \hbar S_{*0}\left[1 - \frac{\Gamma_L}{\hbar k_2} N(\Delta E_{+*})\right] \tag{54}$$

and

$$I_{dir}^{(on)} = I_0 \pi \hbar S_{*0}, \tag{55}$$

represent the steady state values, respectively. The basic difference in the behavior of the direct and sequential current components is as follows: In the off-resonant regime of electron transfer (where $N(\Delta E_{+*}) \ll 1$) the maximal value of the direct switch-on current coincides with its steady state value, $I_{dir}^{(on)} \simeq I_{dir}^{(st)}$. Therefore, a slow kinetic phase is not observed for the direct component. The respective time evolution is determined by the fast single exponential kinetics (see Figs. 7 and 9). This behavior is related to the small population of the charged molecular states. The conclusion is that at an off-resonant regime, the appearance of a large switch-on current

(in comparison to its steady state value) could be only related to one of the sequential components but not to the direct component (compare Figs. 7 and 9 with Fig. 8).

5.2. Resonant regime of charge transmission

The resonant regime of charge transmission is formed if the transmission gaps ΔE_{+*} and ΔE_{-*} become negative. The temporal evolution of the respective current components is represented in the Figs. 10–12. The used light intensity is identical with the one taken for the study of the off-resonant regime.

5.2.1. Single-channel resonant regime

This regime is achieved if $E_* > E_+ + E_F$ or $E_* + E_F > E_-$, i.e. if $\Delta E_{+*} < 0$ or $\Delta E_{-*} < 0$, respectively (cases (c) or (d) of Fig. 6). Physically, the cases $\Delta E_{+*} < 0, \Delta E_{-*} > 0$ and $\Delta E_{+*} > 0, \Delta E_{-*} < 0$ do not differ from each other. Therefore, for the sake of definiteness, let us analyze the case (c). As in the previous subsection, a situation is considered where the fast and the slow kinetic phases are clearly differ from each other. Accordingly, the relaxation of the current components to their steady state values is described by Eqs. (50)–(55) where now $\Delta E_{+*} < 0$ and, thus,

$$S_{*0} = \frac{1}{\hbar\Gamma_L}\left(\Gamma_H^{(1)}\Gamma_L^{(2)} - \Gamma_H^{(2)}\Gamma_L^{(1)}\right),$$
$$Q_{*0} = \frac{1}{\hbar\Gamma_L}\left(\Gamma_H^{(1)}\Gamma_L^{(2)} + \Gamma_H^{(2)}\Gamma_L^{(1)}\right). \tag{56}$$

A comparison of Figs. 10 and 8 shows that the change of ΔE_{+*} from positive values ($\Delta E_{+*} = 0.1$ eV) to negative ones ($\Delta E_{+*} = -0.1$ eV) results in a significant increase of the sequential and distant current components (despite the fact that the width parameters are taken even less than those used in the Figs. 8–10). At the same time, the ratio (52) between the switch-on and the steady state sequential current component is conserved. In the case of the resonant regime, one can also introduce the ratio defined by the direct current component:

$$\eta_{dir} = I_{dir}^{(on)}/I_{dir}^{(st)}. \tag{57}$$

In line with the expressions (54) and (55) it yields $\eta_{dir} = \Gamma_L/\Gamma_H$.If one takes the same relation between the width parameters as it has been used in Fig.8, then $\eta_{dir} \simeq \Gamma_L^{(2)}/\Gamma_H^{(1)} \sim 10$ in correspondence with the exact results depicted in Fig.10.The above given results refer to a current formation connected with the transmission along the channel which is associated with the charged molecular state M_+.The channel includes two types of transmission routs depicted in Fig.6, the left sequential route ($M_* \to M_+ \to M_0$) and the direct tunnel route ($M_* \to M_0$).Analogously, one can consider the current formation if a charge transmission occurs preliminary along the channel related to the molecular charged state M_- (right sequential route $M_* \to M_- \to M_0$ and direct tunnel route $M_* \to M_0$).Recall that the distant rate constants $Q_{*0}^{(12)}$ as well as the $Q_{*0}^{(21)}$ are defined by both charged molecular states M_+ and M_-.To derive respective analytic expressions, one sets $K_{+*} = 0$ in the Eqs.(40), (41), and (22).This results in an analytic form which follows from Eqs.(43) and (55) if one replaces $K_{-*(0)}$ and $K_{*(0)-}$ by $K_{+*(0)}$ and $K_{*(0)+}$, respectively.Our studies show that in this case, the direct current component is comparable with the sequential components (see Fig.11).Since the fast regime of charge transmission is associated now with the hopping of an electron into the HOMO, the maximal value of the sequential current component is less than that of Fig.10 due to the condition$\Gamma_H^{(1)} < \Gamma_L^{(2)}$.

5.2.2. Two-channel resonant regime

This regime is realized if both transmission channels associated with the molecular charged states M_+ and M_- participate in the electron transfer process and if the respective transmission gaps ΔE_{-*} and ΔE_{+*} are negative (cases (d) and (e) in Fig. 6). In this two-channel resonant regime, the left and the right electron transfer channels represented in Fig. 5, give a comparable contribution to the current. The time-dependent evolution of the current components is described by the general expressions (40) and (41) and the set of kinetic equation (34). Fig. 12 does not show any different behavior among the particular currents which belong to a particular channel. The insert of Fig. 12 demonstrates that the fast part of the time evolution completely corresponds to the kinetics of formation of the excited molecular state M_*. The slow part reflects the kinetics at which a population of the charged molecular states M_+ and M_- varies due to a depopulation of the light-induced state M_*. Such a depopulation is negligible during an off-resonant regime of charge transmission but becomes pronounced in the resonance regime.

6. Conclusions

We put forward a detailed study on the time-dependent behavior of light-induced transient currents in molecular junctions, like in a molecular diode **1**-M-**2**. A nonequilibrium set of kinetic equations has been derived for the molecular states which participate in the current formation. Those are the neutral molecular states M_0 and M_* and the two charged molecular states M_+ and M_-. It could be shown that an interelectrode electron transfer $\mathbf{12} \rightleftarrows \mathbf{1}^+\mathbf{2}^-$ takes place along the channels associated with the charged molecular states M_+ and M_-, see Fig. 5. These states participate in a light-induced interelectrode electron transfer in the absence of an applied voltage either as real intermediate states (forming the sequential transmission route) or as virtual intermediate states (forming the direct transmission route). The sequential route includes the hopping of an electron between the molecule and the adjacent electrodes, being thus responsible for a molecular charging. The formation of the respective direct current component is accompanied by the transition of the molecule from its photoexcited state M_* to its ground-state M_0. The time-dependent behavior of the total photocurrent is governed by the molecular populations $P(\alpha; t)$, cf. Eqs. (40) and (41). The latter evolve in line with the kinetic rate Eqs. (34).

The relative efficiency of each route is determined by the actual value of the transmission gaps $\Delta E_{\alpha*}$, ($\alpha = +, -$): If $\Delta E_{\alpha*}$ is positive, then an electron transmission along the M_α-channel proceeds in an off-resonant regime whereas for a negative $\Delta E_{\alpha*}$ the current is formed in the resonant regime. In this regime the sequential and the distant current components significantly exceed the same components formed at the off-resonant charge transmission (see in this context the Figs. 10 and 11 and compare them with the Figs. 7 and 8). In the framework of a HOMO–LUMO model, the direction of the light-induced electron current is determined by the factor $\Gamma_H^{(1)}\Gamma_L^{(2)} - \Gamma_H^{(2)}\Gamma_L^{(1)}$ which reflects the difference between interelectrode electron flow $\mathbf{12} \to \mathbf{1}^+\mathbf{2}^-$ and $\mathbf{1}^-\mathbf{2}^+ \leftarrow \mathbf{12}$.

If the difference between the width parameters $\Gamma_j^{(r)}$ becomes large, a characteristic kinetic effect appears for the transient photo currents. In this case, those currents do exceed their steady state value to a large amount. The physical origin of this effect is related to the fact that the photoexcitation of the molecule ($M_0 \to M_*$ process) initiates a molecular charging (see the schemes in Figs. 4 and 5). Charging is caused by the transition of an electron from the molecule to each electrode ($M_* \to M_+$ process) or from the electrodes to the molecule ($M_* \to M_-$ process). Such a light-induced electron motion forms the fast initial part of the electron transmission which can be seen in the time-dependent behavior of the sequential current components $I_{seq}^{(1)}(t)$ and $I_{seq}^{(2)}(t)$. Molecular recharging is characterized by contact (hopping) rate constants. If

the characteristic recharging time is much less than the characteristic time τ_{st} of the steady state formation, then the maximal value of the transient photocurrent may become rather large compared to its steady state value (see, for instance, Figs. 10 and 12).

Experimental studies of transient photocurrents allow one to clarify the details of contact (molecule–electrode) and distant (electrode–electrode) electron transfer processes in molecular junctions. We have shown that the effective formation of the photocurrent becomes possible if the photon energy $\hbar\omega = E_* - E_0$ exceeds the energy gaps ΔE_{-0} or/and ΔE_{+0}, cf. Fig. 2). This corresponds to an energy level arrangement as shown in the schemes (c)–(f) of Fig. 5.

Acknowledgments

E.G.P. gratefully acknowledge generous support by the Alexander von Humboldt-Foundation. P.H. and V.M. acknowledge the support by the Deutsche Forschungsgemeinschaft (DFG) through priority program DFG-1243 *Quantum transport at the molecular scale* (P. H.) and through the collaborative research center (Sfb) 951 *Hybrid inorganic/organic systems for opto-electronics* (V. M.).

References

[1] F.L. Carter (Ed.), Molecular Electronic Devices, Marcel Dekker, New York, 1982.
[2] A.J. Aviram, Am. Chem. Soc. 110 (1988) 5687.
[3] R.M. Metzger, Acc. Chem. Res. 32 (1999) 950.
[4] A. Nitzan, Annu. Rev. Phys. Chem. 52 (2001) 681.
[5] P. Hänggi, M. Ratner, S. Yaliraki, Chem. Phys. 281 (2002) 111.
[6] C. Joachim, M.A. Ratner, Proc. Natl. Acad. Sci. (USA) 102 (2005) 8800.
[7] G. Cuniberti, G.F. Fagas, K. Richter, Lect. Notes Phys. 680 (2005) 1.
[8] M. Galperin, M.A. Ratner, A. Nitzan, J. Phys. C – Condens. Matter 19 (2007) 103201.
[9] F. Chen, N.J. Tao, Acc. Chem. Res. 42 (2009) 429.
[10] I. Burghardt, V. May, D.A. Micha, E.R. Bittner (Eds.), Energy Transfer Dynamics in Biomaterial Systems, Springer-Verlag, Berlin, 2009.
[11] V. Mujica, M.A. Rarner, A. Nitzan, Chem. Phys. 281 (2002) 147.
[12] C.B. Winkelmann, I. Ionica, X. Chevalier, G. Royal, C. Bucher, V. Bouchiat, Nano Lett. 7 (2007) 1454.
[13] A.S. Kumar, T. Ye, T. Takami, B.-C. Yu, A.K. Flatt, J.M. Tour, P.S. Weiss, Nano Lett. 8 (2008) 1644.
[14] S.J. van der Molen, J. Liao, T. Kudernac, J.S. Agustsson, L. Bernard, M. Calame, B.J. van Wees, B.L. Feringa, C. Schönenberger, Nano Lett. 9 (2009) 76.
[15] X.H. Qui, G.V. Nazin, W. Ho, Science 299 (2003) 542.
[16] A.J. Gesquiere, S. Park, P.F. Barbara, J. Chem. Phys. B 108 (2004) 10301.
[17] Z.-C. Dong, X.-L. Guo, A.S. Trifonov, P.S. Dorozhkin, K. Miki, K. Kimura, S. Yokoyama, S. Mashiko, Phys. Rev. Lett. 92 (2004) 086801.
[18] M. Pivetta, Physics 3 (2010) 97.
[19] J. Lehmann, S. Kohler, P. Hänggi, A. Nitzan, Phys. Rev. Lett. 88 (2002) 228305.
[20] J. Lehmann, S. Camalet, S. Kohler, P. Hänggi, Chem. Phys. Lett. 368 (2003) 282.
[21] J. Lehmann, S. Kohler, P. Hänggi, A. Nitzan, J. Chem. Phys. 118 (2003) 3283.
[22] M. Galperin, A. Nitzan, J. Chem. Phys. 124 (2006) 234709.
[23] B.D. Fainberg, M. Jouravlev, A. Nitzan, Phys. Rev. B 76 (2007) 245329.
[24] B.D. Fainberg, M. Sukharev, T.H. Park, M. Galperin, Phys. Rev. B 83 (2011) 205425.
[25] J. Buker, G. Kirczenow, Phys. Rev. B 78 (2008) 125107.
[26] J. Lehmann, S. Kohler, V. May, P. Hänggi, J. Chem. Phys. 121 (2004) 2278.
[27] S. Kohler, J. Lehmann, P. Hänggi, Phys. Rep. 406 (2005) 379.
[28] S. Kohler, P. Hänggi, Nat. Nanotechnol. 2 (2007) 675.
[29] I. Franco, M. Shapiro, P. Brumer, Phys. Rev. Lett. 99 (2007) 126802; I. Franco, M. Shapiro, P. Brumer, J. Chem. Phys. 128 (2008) 244906.
[30] F.J. Kaiser, P. Hänggi, S. Kohler, New J. Phys. 10 (2008) 1.
[31] S. Welack, M. Schreiber, U. Kleinekathöfer, J. Chem. Phys. 124 (2006) 044712.
[32] G.-Q. Li, M. Schreiber, U. Kleinekathöfer, Europhys. Lett. 79 (2007) 270006.
[33] V. May, O. Kühn, Nano Lett. 8 (2008) 1095.
[34] E.G. Petrov, M.V. Koval, Phys. Lett. A 372 (2008) 5651.
[35] A.I. Akhiezer, S.V. Peletminsky, Methods of Statistical Physics, Pergamon Press, Oxford, 1981.
[36] K. Blum, Density Matrix Theory and Application, second ed., Plenum Press, New York, 1996.
[37] V. May, O. Kühn, Charge and Energy Transfer Dynamics in Molecular Systems, second ed., Wiley-VCH, Weinheim, 2004.
[38] E.G. Petrov, Ye.V. Shevchenko, V. May, P. Hänggi, J. Chem. Phys. 134 (2011) 204701.
[39] E.G. Petrov, Chem. Phys. 326 (2006) 151.
[40] E.G. Petrov, V. May, P. Hänggi, Phys. Rev. B 73 (2006) 045408.
[41] V. May, O. Kühn, Phys. Rev. B 77 (2008) 115439.
[42] E.G. Petrov, Ukr. J. Phys. 56 (2011) 721.
[43] A.S. Davydov, Quantum Mechanics, secod ed., Pergamon Press, Oxford, 1976.
[44] M. Leijnese, M.R. Wegewijs, M.H. Hettler, Phys. Rev. Lett. 103 (2009) 156803.
[45] L.I. Glazman, M. Pustilnik, in: H. Bouchiat, Y. Gefen, S. Gueron, G. Montambaux, J. Dalibard (Eds.), Nanophysics: Coherence and Transport, Elsevier, Amsterdam, 2005. p. 427.
[46] E.G. Petrov, V. May, P. Hänggi, Chem. Phys. 319 (2005) 380.
[47] E.G. Petrov, Mol. Cryst. Liq. Cryst. 467 (2007) 3.
[48] E.G. Petrov, Ya.R. Zelinskyy, V. May, P. Hänggi, Chem. Phys. 328 (2006) 173.
[49] L. Wang, V. May, Chem. Phys. 375 (2010) 252.
[50] A. Aviram, M.A. Ratner, Chem. Phys. Lett. 29 (1974) 277.
[51] R. Volkovich, U. Peskin, Phys. Rev. B 83 (2011) 033403.
[52] Y. Meir, N.S. Wingreen, P.A. Lee, Phys. Rev. Lett. 66 (1991) 3048.
[53] Y. Meir, N.S. Wingreen, P.A. Lee, Phys. Rev. Lett. 70 (1993) 2601.
[54] M.H. Hettler, H. Schoeller, W. Wenzel, Europhys. Lett. 57 (2002) 571.
[55] The wide-band approximation [4] is valid for electrodes fabricated from the noble metals. In this case, the width parameter (23) can be chosen as not exhibiting a dependence on the transmission energy E.
[56] While the current unit is given in Amperes one has to set $\hbar \simeq 6.58 \cdot 10^{-16}$ eV · s. This means that the quantities $\hbar K_{\alpha\alpha'}, \hbar Q_{*0}^{(rr')}$, and the width parameters $\Gamma_j^{(r)}$ are taken in eV.